INTENSE-BEAM ISSUES IN CSNS AND C-ADS ACCELERATORS

Shinian Fu, Jingyu Tang, Sheng Wang, Zhihui Li, Jun Peng, Fang Yan, Shouxian Fang
Institute of High Energy Physics, Beijing 100049, China

Abstract

In 2011 construction of two intense-beam accelerators were launched for China Spallation Neutron Source (CSNS) project and China Accelerator Driven System (C-ADS) project. CSNS uses a pulsed accelerator with an H^- linac and a proton rapid cycling synchrotron, and C-ADS has a CW proton linac with superconducting cavities. In both cases, the beam power is high and beam loss control is a key issue in beam dynamics. Beam emittance growth and beam halo formation must be carefully studied in beam dynamics and well controlled in machine design. This paper will present a brief introduction to the physics design of the two intense-beam accelerators, especially on the issue of beam instability. In their linac design equapartitioning focusing scheme is adopted to avoid coupling instability. Some beam halo formation experimental results due to mismatching will be compared with simulations. Beam halo generation due to the quench of superconducting cavity and magnet is investigated in detail and compensation scheme is also proposed. Some code development are presented.

INTRODUCTION

High intensity proton accelerators have majorly two important applications in China at present: one is for China Spallation Neutron Source and another is for China Accelerator Driven System[1]. The both projects have been formally launched in 2011. The two accelerators impose a great challenge to Chinese accelerator community in terms of not only key technology, but also beam dynamics.

The CSNS is designed to accelerate proton beam pulses to 1.6 GeV kinetic energy at 25 Hz repetition rate, striking a solid metal target to produce spallation neutrons The accelerator provides a beam power of 100 kW on the target in the first phase and then 500 kW in the second phase by increasing the average beam intensity 5 times while raising the linac output energy. A schematic layout of CSNS phase-1 complex is shown in Figure 1. In the phase one, an H^- ion source produces a peak current of 25 mA H^- beam. RFQ linac bunches and accelerates it to 3 MeV. DTL linac raises the beam energy to 80 MeV. After H^- beam is converted to proton beam via a stripping foil, the RCS accumulates and accelerates the proton beam to 1.6 GeV before extracting it to the target. Phase-I has a budget of $260 M for construction of the accelerator, the spallation neutron target and 3 neutron spectrometers. Its site is at Dongguan, south part of China. The local government will support free land, additional budget of $57M, infrastructure, dedicated high-way and power transformer station. The project is expected to be accepted for user operations in the first half of 2018.

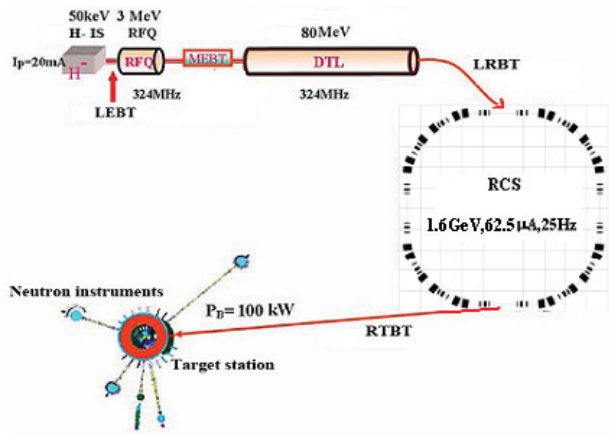

Figure 1:Schematic layout of CSNS facility.

In 2011 a Chinese roadmap for long-term development of ADS was proposed by Chinese Academy of Sciences. It outlines a three-step plan with a small test setup, an experimental facility and a demonstration facility in a period from 2011 to 2032，as plotted in Figure 2.

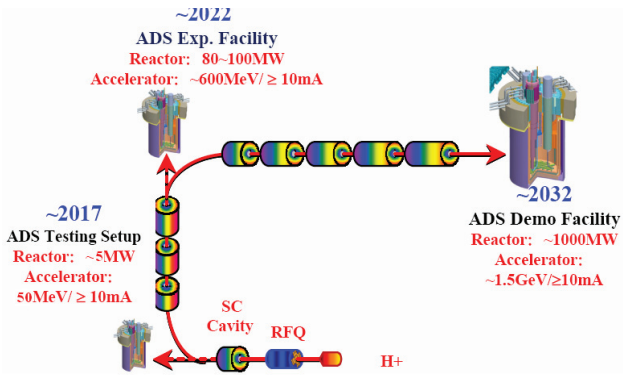

Figure 2: Roadmap of ADS development in China.

The C-ADS proton linac will operate in CW mode with a high average current of 10mA. Superconducting cavity is the best option, except for the front-end. In our preliminary design the 1.5 GeV linac consists of two injectors, two spoke cavity sections and two elliptical cavity sections. In operation, only one injector runs and another is hot standby for a high reliability which is a key requirement for the target and reactor.

ISBN 978-3-95450-118-2

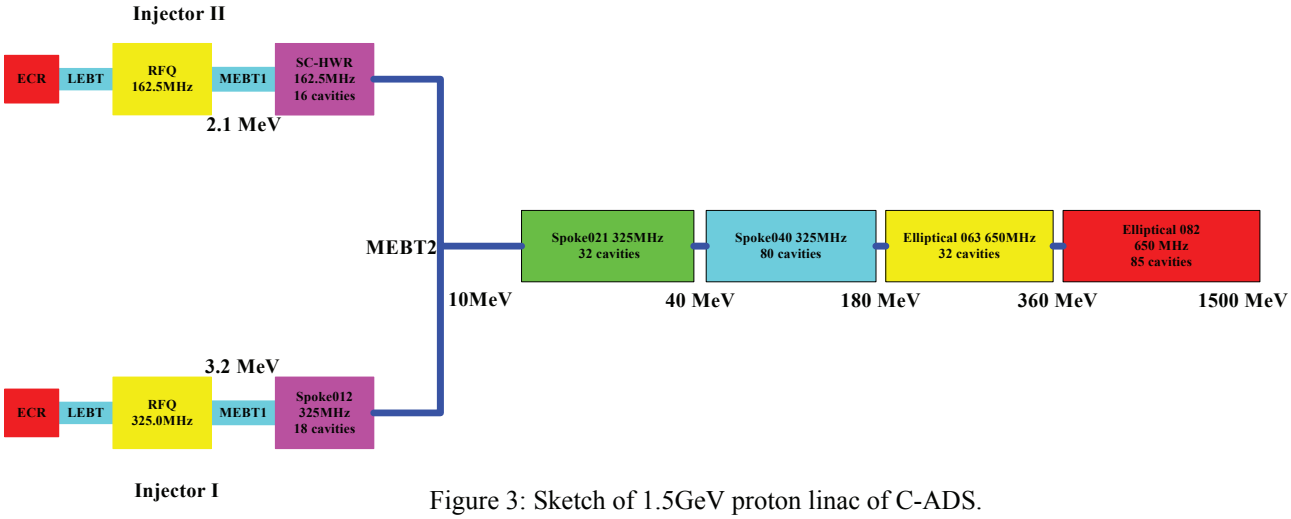

Figure 3: Sketch of 1.5GeV proton linac of C-ADS.

To explore different technology at present, the two injectors have different design: the Injector-I is mainly composed with an ECR ion source, a 3.2 MeV room temperature RFQ at 325 MHz and superconducting spoke cavities at 325 MHz; while the Injector-II mainly consists of an ECR ion source, a 2.1 MeV room-temperature RFQ at 162.5 MHz and superconducting HWR cavities at 162.5 MHz. Ten MeV proton beam from the injectors will be matched via an MEBT2 with the following main linac, as shown in Figure 3.

BEAM LOSS STUDY ON CSNS ACCELERATOR

Beam loss control is a major concern for CSNS accelerator in beam dynamics design, as it is a bottleneck for beam power increase for this high intensity machine. In its linac design, emittance growth and beam halo formation are recognized as the source of the beam loss, expect for the beam loss from errors. For the rapid cycling synchrotron, it was found that the beam loss is related to space charge effect, beam instability due to impedance, resonance due to magnet errors, in addition to the longitudinal RF capture losses.

Equipartitioning Design of CSNS Linac

The linac accelerates a pulsed beam of 15mA to 80MeV in the first phase and of 30mA to 250MeV in the second phase. The major parameters of the linac is given in Table 1 for the two phases. In the beam dynamics design, the beam current for the second phase is adopted.

Table 1: CSNS Linac Parameters in Two Phases

Parameters	Phase-I	Phase-II
Particle	H-	H-
Beam energy (MeV)	80	250
Pulse current (mA)	15	30
RF frequency(MHz)	324	324
Macropulse duty factor(%)	1.05	2.63
Repetition rate(Hz)	25	25
Chopping rate (%)	50	50
Main structure	DTL	DTL+SC

DTL is the main linac which accelerates beam from 3MeV to 80MeV in the first phase. The DTL linac was re-designed and we changed lattice from FD to FFDD with a larger bore radius. This change comes from the end-to-end simulations with the real beam distribution of the RFQ output and with various errors of the machine. These simulations reach a conclusion that the FD lattice has more beam loss than FFDD lattice, majorly because of its smaller bore radius. To avoid the structure instability in high current linac we designed σ_{x0}, σ_{z0} <90°, where σ_{x0} and σ_{z0} are the zero-current phase advance in transverse and longitudinal directions. To avoid the emittance growth induced by the coupling instability between transversal and longitudianl directions in a space-charge dominated beam bunch, the transverse and longitudinal beam temperatures has been designed to keep equal according to the equipartitioning theory [2]:

$$\frac{T_{\perp}}{T_{\parallel}} = \frac{k_x \varepsilon_{nx}}{k_z \varepsilon_{nz}} = \gamma_0^2 \frac{\varepsilon_{nx}^2}{\varepsilon_{nz}^2} \cdot \frac{z_m^2}{a^2} = 1$$

here, ε_x and ε_z are the normalized RMS emittances of the transverse and longitudinal phase spaces, a and z_m are the radii of the bunch in the transverse and longitudinal directions, γ_0 is the relativistic parameter. Applying this formula to the FFDD lattice design of the DTL linac, we got the zero current phase advance per period as shown in Figure 4.

ISBN 978-3-95450-118-2

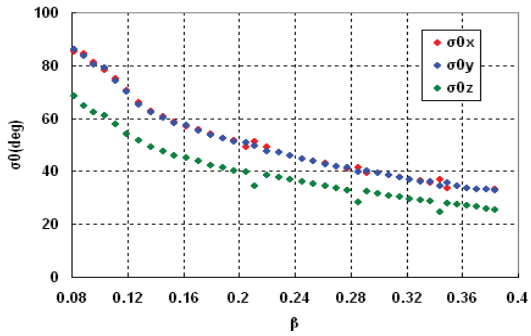

Figure 4: Designed zero current phase advance in three directions for equipartitioning DTL linac.

The beam emittance growth is effectively minimized by the equipartitioning scheme in Figure 5 indicates that the emittance increases less than 12% in transversal directions in the CSNS DTL of 30mA beam current with the equipartitioning lattice design, much less than that of constant zero-current phase advance design scheme. The major transversal emittance growth in the linac happens in the section of MEBT, which is larger than 28%.

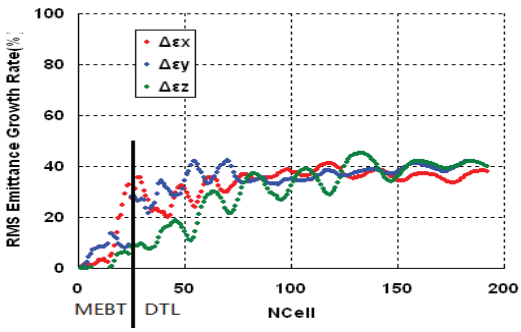

Figure 5: Emmitance growth rate in the CSNS linac with equipartitioning lattice in the DTL.

Beam Loss Control in CSNS RCS

Figure 6 shows the layout of the RCS ring. The ring adopts a hybrid lattice with missing-dipole FODO arcs and doublet straights. The FODO arcs allow easy lattice optics correction. The 4 m gap created by the missing dipole near the maximum dispersion location allows efficient longitudinal collimation. Table 2 lists the major design parameters of the RCS in the first phase.

As the beam power is rather high in the ring, the beam loss must be tightly controlled so as to reach less than 1 W/m lost beam power in average along the ring. To this end, several measures are taken in the design[3]: such as optimising the lattice design to avoid resonance due to magnet errors, pre-chopping the injection beam pulse for a high capture in ring RF bucket, phase-space painting the injection beam for a low space-charge tune spread, optimising the RF field and synchronous phase for a high capture rate and low longitudinal emittance growth, designing a large aperture and minimizing errors. In addition to these measures, localization of beam losses at the radiation-protected elements is also designed by means of collimators. Transversal collimators for scrapping halo particles will be set up in the first phase while the momentum collimation is designed for the CSNS phase-II. The transversal collimators have an acceptance of 350 πmm·mrad.

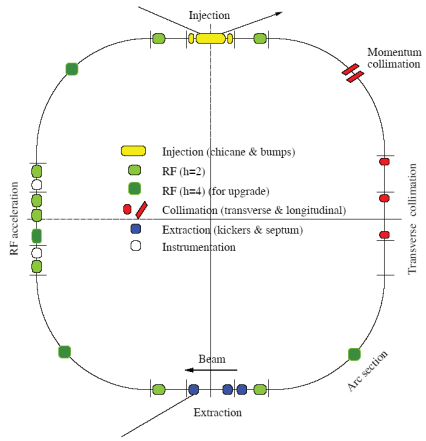

Figure 6: Functional layout of the CSNS RCS.

Table 2: The Major Design Parameters of the CSNS RCS

Parameters	Unit	Value
Inj./Ext. energy	GeV	0.08/1.6
Circumference	m	228
Beam population	$\times 10^{13}$	1.56
Harmonic number	*h*	2
RF frequency	*MHz*	1.02-2.44
Repetition frequency	Hz	25
Betatron tune	ν_x/ν_y	4.86/4.78
Chromaticity	*h/v*	-4.3/-8.2
Trans. acceptance	πmm·mrad	540

Studies on beam instability due to impedance are the essential work in CSNS RCS beam dynamics design. The impedance calculation on various ring components has been conducted. The results indicate that impedances of the RCS mainly come from resistive wall, steps, RF cavities, collimators, bellows, vacuum pumps, flanges, extracted kickers, and et al. It is found that the transversal resistive wall impedance is most likely to appear in the ring. Theoretical calculation and multi-particle simulation of the CSNS phase-I give a growth time of about 5ms, much less than 20 ms of beam stored time in the ring. The resistive wall instability is more serious at the low-energy end of each cycle. And it becomes much more serious in

ISBN 978-3-95450-118-2

the 500 kW upgrade, as the growth time will be less than 2 ms. However, it is found that the natural chromaticity leading the tune spread can suppress resistive wall instability in CSNS/RCS, as shown in Figure 7.

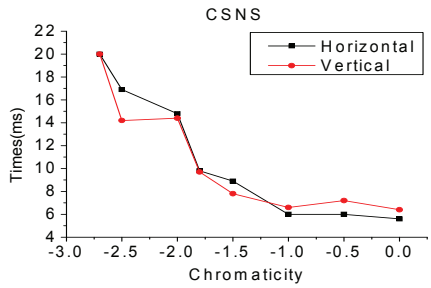

Figure 7: Resistive wall instability growth time dependence on the natural chromaticity in CSNS RCS.

BEAM LOSS CONTROL STUDY IN THE C-ADS LINAC

For C-ADS, as a CW high current linac, beam loss control is very challenging task in the beam dynamics design. The linac mainly consists of superconducting cavities with different geometrical β, as shown in Figure 3. Different transversal focusing lattice is adopted in the linac. In the section of spoke cavity, superconducting solenoid inside the cryomodule forms a transversal focusing lattice, so as to get a short focusing period with a strong focus to the low energy beam. As the beam energy becomes higher in the section of elliptical cavity, room temperature quadrupole triplet is adopted between the cryomodules. The lattice is designed with the zero-current phase advance in the three directions is less than 90° to avoid structural resonance in beam envelope. The equipartitioning scheme is applied in the main linac, i.e. from 10 MeV to 1.5 GeV. For the emittance ratio $\varepsilon_{nz}/\varepsilon_{nt}$ = 0.85, we set the working point a little bit deviating from it, with k_{z0}/k_{x0} = 1.33, instead of 1.18 which corresponds to $\varepsilon_{nz}/\varepsilon_{nt}$ = 0.85, as shown with the solid line in Hofmman chart of Figure 8. By this way the working point can get more far from the dangerous resonant point.

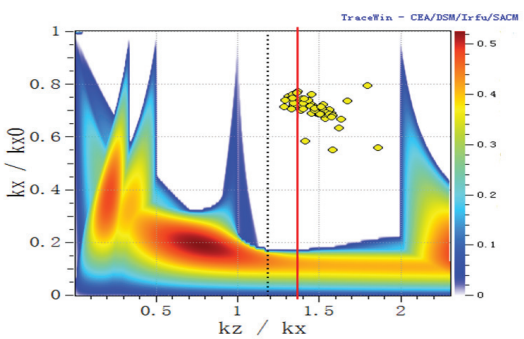

Figure 8: Hofmman chart for C-ADS linac.

To avoid the mismatching at the structure transition points, cavity field and synchronous phase, as well as the adjacent focusing elements are slightly adjusted to reach a better match. Multiparticles simulation for the baseline design of the main linac results in an emittance growth in x-plane less than 60%, y-plane less than 50% and z-plane less than 50%. Baseline design has no particle loss in the simulation. However, the actual machine has many types of errors and the input beam distribution is not ideal. Especially, for the superconducting linac, the quench failures of the cavity and the solenoid will also result in emittance growth and beam losses. A series of compensation schemes for the failure has been investigated. The cavity accelerating field design we leave a margin of 50% for compensation in case of one cavity failure. According to the simulations, one solenoid failure after the first spoke cavity at the low energy end of the main linac will cause a lot of beam losses. The lost beam has a power about 2 kW along less than half meter beam line. And the maximum growth of RMS emittance is about 3.7 times. It is found the emittance increases not only in transversal direction, but also in longitudinal direction. Simulation identified that the reason is the nonlinear transversal field coupling to the longitudinal direction, rather than the space-charge effect. Various compensation schemes were compared for better re-matching of the beam. One proposal is to tune the nearby solenoids to re-match the beam with the following focusing channel. But it can only compensate for the transversal mismatching. A better scheme is to tune the nearby cavity, in addition, to re-match the beam longitudinally. Figure 9 shows the longitudinal phase space at the exit of the linac. From the figure one can see that a nonlinear tail is obvious in the phase space if only transversal compensation is applied in the left plot. The tail disappears when the longitudinal compensation is added in the right plot.

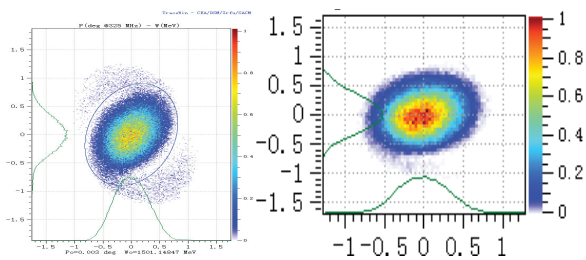

Figure 9: Longitudinal phase space; left: with transversal compensation only; right: plus a longitudinal compensation.

EXPERIMENTAL BEAM HALO STUDY

An intense-beam proton RFQ was built at IHEP in 2006. Its output beam energy is 3.5 MeV with an average beam current of 3 mA. Following the RFQ, a dedicated beam line was set up for the beam halo experimental study[4]. The beam line consists of FODO lattice with 24 quadrupoles and a section for beam mismatch tuning with 4 quadrupoles. 14 scanners are arranged along the beam line for beam profile monitor by wires and beam halo

ISBN 978-3-95450-118-2

detection by scraper. For the matched beam, we found the measured bean profile is coincident with the simulation, but for the mismatched beam with mismatch factor μ=2, there is a prominent difference between measurement and simulation. The measured beam profile exhibits a "shoulder", as shown in Figure 10. This is only a preliminary result . More experimental study is going on.

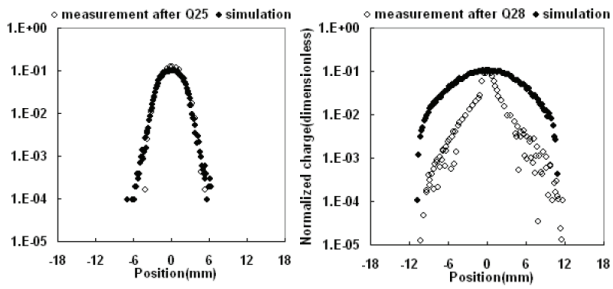

Figure 10: Measured and simulated beam profiles for matched beam(left) and mismatched beam(right) with mismatch factor μ=2.

CODE DEVELOPMET

The DTL linac, in fact, is not a periodical focusing channel because some machine parameters are keeping change along the linac, such as cell-length, the synchronous phase and accelerating field, and the beam parameters such as emittance and bunch shape also change. As a result, when one apply the theoretical equipartitioning formula to the lattice design, these parameter variation can not be taken into account. For this reason, we see in Hofmann stability chart the designed linac has a trace of the working point, and unfortunately some time it may get into unstable region, resulting in an exchange of beam thermal energy [5].

To deal with this issue, we explored the function of the TRACE3-D code, so that the equipartitioning parameter can keep very close to unit along the whole linac[6]. Figure11 shows an example of the application of the code to a DTL section. Unfortunately, as we have no the Window version of TRACE3-D source code, it is a UNIX version and inconvenient for user.

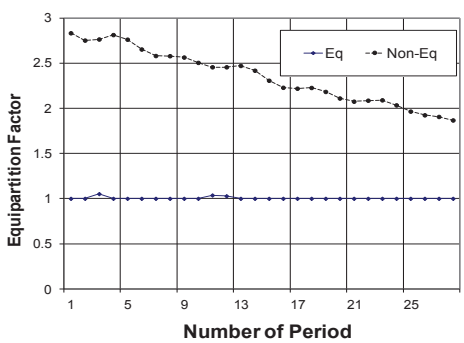

Figure 11: Modified TRAC3-D code to design a full equipartioning DTL.

TraceWin code was used for the C-ADS failure compensation study. This code can .correctly compensate for the energy loss due to cavity failure, but not correctly for the arrival time at the matching point, as it can automatically fit the RF phase for the downstream cavities without taking account of the energy loss in the failure cavity. As we have no the source code of TraceWin, an additional code was developed for the cavity compensation scheme study on the platform of Mathlab.

3-D space charge effect plays an important role in high intensity beam dynamics, especially for the study on the coupling resonance. To reach a faster simulation of 3D space-charge effect in multi-particle simulation, a linac design and simulation code is under development with FFT solver of the space charge force[7]. he technology development during the past several years in the field of high intensity proton accelerators.

ACKNOWLEDGEMENTS

The authors thank the accelerator team members of the CSNS and C-ADS projects for their nice collaborations and great contribution.

REFERENCES

[1] Shinian Fu, Hesheng Chen, Yunlong Chi, Shouxia.n Fang, Li Ma, Weimin Pan, Jingyu Tang, Chuang Zhang, Yuan He, Hongwei Zhao, Chinese Plans for ADS and CSNS, Proceedings of SRF2011, Chicago, (2011).

[2] Hofmann, et al., Space charge resonances in two and three dimensional anisotropic beams, Phys. Rev. ST Accel. Beams 6, 024202 (2003).

[3] J. Tang, S.Fu, L.Ma, Proc. of HB2010, Sept. 2010, Morschach, Switzerland, p.38 (2010).

[4] Peng Jun, Huang Tao, Liu Hua-Chang, et al., The Beam Halo Experiment at IHEP, Chinese Physics (C), to be published.

[5] Yin Xuejun, Fu Shinian, Peng Jun, Chinese Physics (C), 33 (9): 811-814(2009) .

[6] Fu Shinain, Guan Xialing, Fang Shoxian, HEP & NP, 26 (01): 79-86(2002) .

[7] Zhao Ya-Liang, Fu Shi-Nian, Li Zhi-Hui, Xu Cheng-Hai, Yang Xiao-Yu, 3D Space Charge Code with FFT Method, Chinese Physics (C), to be published.

ISBN 978-3-95450-118-2